Ceramics International **24** (1998) 483–487

PII: S0272-8842(97)00037-0
0272-8842/98 $19.00+.00

Nanoprecipitation in Al_2O_3–3 mol%Ti_2O_3 Due to Oxidation

A. Yasuda,[†] J. Aoki[‡] & T. Sakuma*

Department of Materials Science, Faculty of Engineering, The University of Tokyo, Tokyo 113, Japan

(Received 20 January 1997; accepted 7 April 1997)

Abstract: The solubility of Al_2O_3–Ti_2O_3 is determined with X-ray diffraction analysis. On the basis of the solubility data, the precipitation from supersaturated Al_2O_3–3 mol%Ti_2O_3 solid solutions is examined. The precipitation is strongly dependent on ageing atmosphere. Coarse precipitates of Ti_2O_3 are formed in matrix after ageing at 1100°C in a reduced atmosphere of Ar–5%H_2. In contrast, intragranular nanoprecipitates of 20∼80 nm in size are generated during ageing in air at 1100°C along with fairly large grain boundary precipitates of TiO_2 with a rutile structure. The nanoprecipitates have an ordered corundum structure, and are coherent with α-Al_2O_3 matrix. Nanoprecipitation must occur in Al_2O_3–Ti_2O_3 by oxidation probably due to the very limited solubility of Ti^{4+} ions in α-Al_2O_3 in comparison with Ti^{3+} ions. © 1998 Elsevier Science Limited and Techna S.r.l.

1 INTRODUCTION

It is well-known that ceramic nanocomposites have excellent mechanical properties such as hardness, strength, fracture toughness at room temperature. One of the most famous processes is to produce Si_3N_4/SiC nanocomposites from amorphous Si–N–C powders prepared with CVD method.[1] Nanocomposites are also fabricated by conventional sintering.[1–3] An example of such composites is Al_2O_3–10 vol%SiC, in which SiC particles with a size of 80 nm are embedded in Al_2O_3 grains with about 1 μm in size due to Al_2O_3 grain growth during sintering.[2] It is also possible to get nanocomposites by annealing in a reduced atmosphere.[4–7] In Al_2O_3–Cr_2O_3, for example, Cr precipitates are formed during annealing in a reduced atmosphere because Cr is almost insoluble in Al_2O_3 in contrast with Cr_2O_3.[5] The atmosphere control technique must be effective to form nanoprecipitates in alumina–titania because the solubility of TiO_2 in Al_2O_3 is much smaller than that of Ti_2O_3.[8,9]

This paper aims to report the nanoprecipitation from Al_2O_3–3 mol%Ti_2O_3 solid solutions after ageing at 1100°C in an oxidised atmosphere.

2 EXPERIMENTAL PROCEDURE

High-purity commercial Al_2O_3 powders (>99.99%: Taimei chemicals-TM-DAR) and Ti_2O_3 powders (>99.9%: rare-metallic) were used for starting materials. Al_2O_3 powders containing up to 5 mol% Ti_2O_3 were mixed in a ball mill for 24 h using Al_2O_3 ball and ethanol. They were dried in an oven, crushed into powders to pass through 250 μm seive and then uniaxially compacted into 5 mm×5 mm×20 mm in size under a pressure of 40 MPa. The green compacts were further cold-isostatically pressed at 125 MPa. They were sintered at a temperature between 1300 and 1700·C for 2 h in a reduced atmosphere of Ar–5%H_2 gas flow at 1 atm using a halogen lamp image furnace (Shinkuriko, MIRO). Temperature was controlled within an accuracy of ±1°C. Heat treatment was

*To whom correspondence should be addressed.
[†]Present address: Sony Corporation, Atsugi Technology Center, Japan.
[‡]Present address: Nippon Steel Corporation, Muroran Works, Japan.

made at 1100°C in a reduced or oxidised atmosphere. Samples for heat treatment were sliced into plates with about 260 μm thickness using diamond saw. Phase determination and lattice constant measurements were made with X-ray diffraction (XRD) analysis using Mac Science-MXP18 operated at 40 mA and 200 kV with a Ni-filtered Cu-Kα radiation. Calibration was made using high-purity Si standard powders, and lattice constants were estimated from least-square method employing $\{13\bar{4}\underline{10}\}$, $\{30\bar{3}\underline{12}\}$, $\{20\bar{2}\underline{14}\}$, $\{14\bar{5}\underline{6}\}$, $\{11\bar{2}\underline{15}\}$, $\{40\bar{4}\underline{10}\}$ reflections of α-alumina. Disc samples were polished into 10–50 μm thickness, and then ion-milled to get thin foils for electron microscopy on a liquid nitrogen-cooled stage so as to inhibit specimen damage. They were examined with transmission electron microscopy TEM: HITACHI, H800) or with . high-resolution electron microscopy (HITACHI, H9000NAR attached with EDS spectrometer).

3 RESULTS AND DISCUSSION

Figure 1 is the XRD profiles in Al_2O_3–3 mol%-Ti_2O_3. The peaks from α-Al_2O_3 and from Ti_2O_3 with a corundum structure appear in the profile of raw powders (Fig. 1(a)), but the peaks from Ti_2O_3 almost completely disappear and only α-Al_2O_3 peaks are observed in the sample sintered at 1600°C for 2 h in a reduced atmosphere of Ar-5%H_2 (Fig. 1(b)). The peaks from α-Al_2O_3 in the sintered sample slightly shift towards low 2θ angles. Ti_2O_3 must be in solution in Al_2O_3 with a corundum structure, and the lattice constant of corundum structure becomes larger. As in Fig. 1(c), the sample aged at 1100°C for 24 h in a reduced atmosphere of Ar–5%H_2 exhibits the weak peaks from Ti_2O_3 along with the major peaks from α-Al_2O_3. This is a result of precipitation of Ti_2O_3 during ageing. In contrast, the peaks from TiO_2 with rutile structure are observed as well as the major α-Al_2O_3 peaks in the sample aged at 1100°C for 24 h in air (Fig. 1(d)). The precipitation is influenced by ageing atmosphere.

Figure 2 shows the unit cell volume of corundum structure estimated from the peaks of α-Al_2O_3 as a function of Ti_2O_3 content. The temperatures shown in Fig. 2 are the heating temperatures. From the data of Fig. 2, the solubility of Ti_2O_3 in Al_2O_3 is determined to be 1.3, 2.0, 3.0, and 3.7 mol% at 1400, 1500, 1600 and 1700°C, respectively. The solubility limit is plotted in Fig. 3 together with the previous data.[9] The present data exhibit larger solubility than the previous ones.

Figure 4 is the electron micrographs of Al_2O_3–3mol%Ti_2O_3. The micrograph of Fig. 4(a) is obtained in the sample sintered at 1600°C for 2 h in Ar–5%H_2 atmosphere, in which no precipitates are found. Ti_2O_3 must be dissolved into α-Al_2O_3 matrix during sintering at 1600°C. This fact means

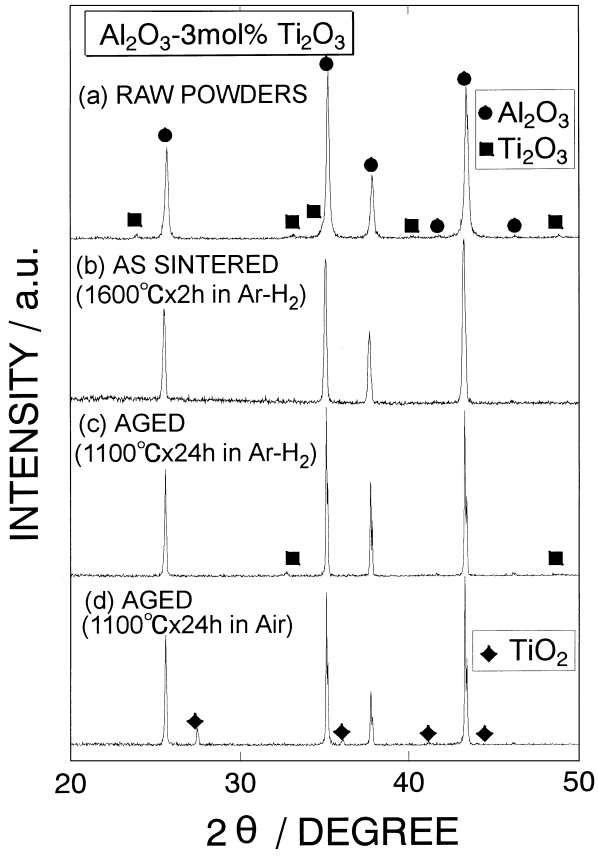

Fig. 1. XRD profiles of Al_2O_3–3 mol%Ti_2O_3; (a) raw powders, (b) the sample sintered at 1600°C for 2 h in Ar–5%H_2, (c) the sample aged at 1100°C for 24 h in Ar– 5%H_2, and (d) the sample aged at 1100°C for 24 h in air.

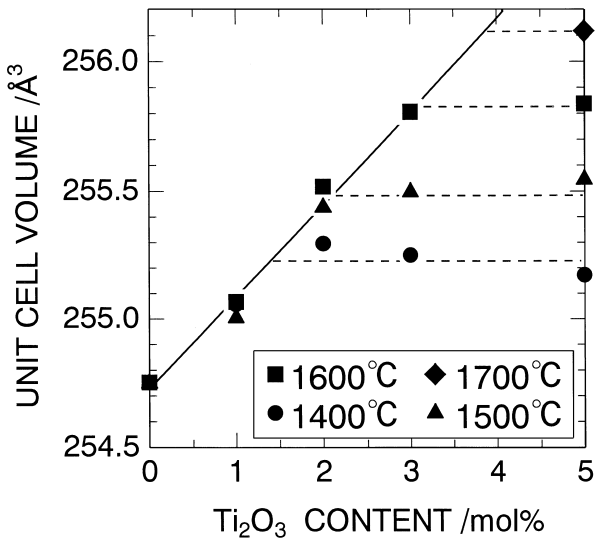

Fig. 2. The unit cell volume of corundum structure in Al_2O_3–Ti_2O_3 as a function of Ti_2O_3 content. The data are obtained in samples annealed at four temperatures between 1400 and 1700°C.

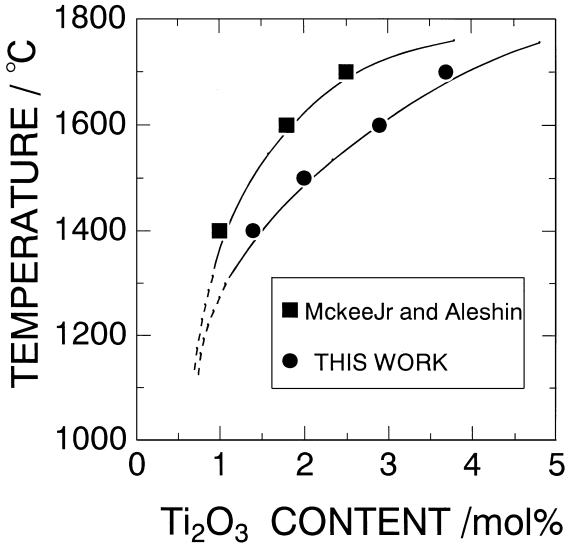

Fig. 3. The solubility limit of Ti_2O_3 in α-Al_2O_3. The solubility data reported by McKee Jr and Aleshin[8] are also shown for comparison.

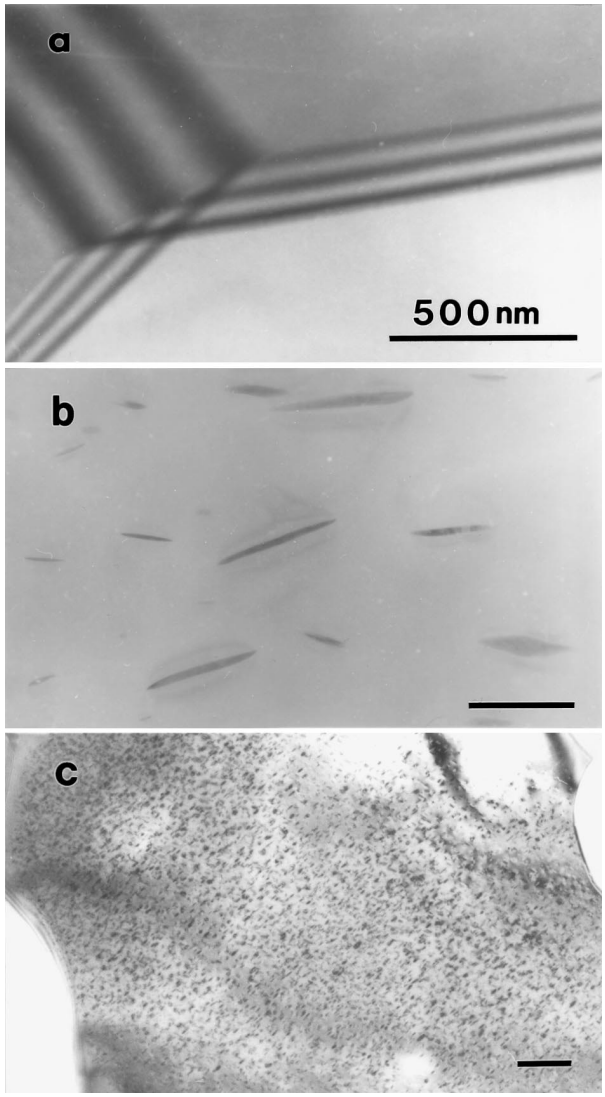

Fig. 4. TEM micrographs of Al_2O_3–3 mol% Ti_2O_3; (a) sintered at 1600°C for 2 h, (b) aged at 1100°C for 24 h in Ar–5% H_2, and (c) aged at 1100°C for 24 h in air. The bars in the micrographs represent 500 nm.

that the solubility of Ti_2O_3 in α-Al_2O_3 is larger than 3 mol% at 1600°C. The result is in agreement with our solubility data rather than the previous ones.[9] A low density of coarse precipitates with a size of about 500 nm are formed in the sample aged at 1100°C for 24 h in Ar–5% H_2 atmosphere as in Fig. 4(b). They are Ti_2O_3 precipitates formed during ageing. On the other hand, the sample aged at 1100°C for 24 h in air has a high density of precipitates with a size of 20~80 μm inside grains together with coarse grain boundary precipitates (Fig. 4(c)). The coarse grain boundary precipitates are TiO_2 with a rutile structure, while nanoprecipitates in matrix are not TiO_2 but have a crystal structure similar to α-Al_2O_3 as will be discussed later. The size and density of nanoprecipitates change little after prolonged ageing up to 200 h at 1100°C in air. The nanoprecipitates are very stable even at high temperatures.

Figure 5 shows the bright-field and dark-field images of nanoprecipitates in Al_2O_3–3 mol% Ti_2O_3 aged at 1100°C for 24 h in air. Since the precipitates exhibit a variety of contrasts, it is not possible to make clear their structural details but several interesting features are revealed in Fig. 5. The nanoprecipitates seem to develop in three directions in Fig. 5(a). From the trace analysis of the precipitates, the habit plane is determined to be $\{10\bar{1}4\}$ of alumina matrix. Two sets of the precipitates are brightly imaged in Fig. 5(b) and (c), which are taken with the reflections of b and c in Fig. 5(d), respectively. The extra spots from the precipitates accompany the streaks normal to the habit planes. They are not indexed from rutile structure, but from an ordered corundum structure. Titanium ions may be ordered in the precipitates.

A nanoprecipitate is taken with a higher magnification in Fig. 6. The precipitate is coherent with matrix, and accompanies the $\{10\bar{1}4\}$ fault planes (Fig. 6(a)). Figure 6(b) and (c) are the results of TEM–EDS analysis in matrix and the precipitate, respectively. Titanium peaks appear only from the precipitates, not from the matrix. The nanoprecipitates with an ordered corundum structure must be a metastable phase. However, they are very stable, and do not grow rapidly during high-temperature ageing. The growth rate is different between Ti_2O_3 precipitates and the nanoprecipitates. The stability of nanoprecipitates may arise from the fact that titanium ions in the precipitates are tetravalent, because the solubility of Ti^{4+} is extremely small in α-Al_2O_3,[9] and the diffusional growth of precipitates is dependent on the solubility of relevant ions.[10,11] However, it should be noted that the oxidation of titanium ions from

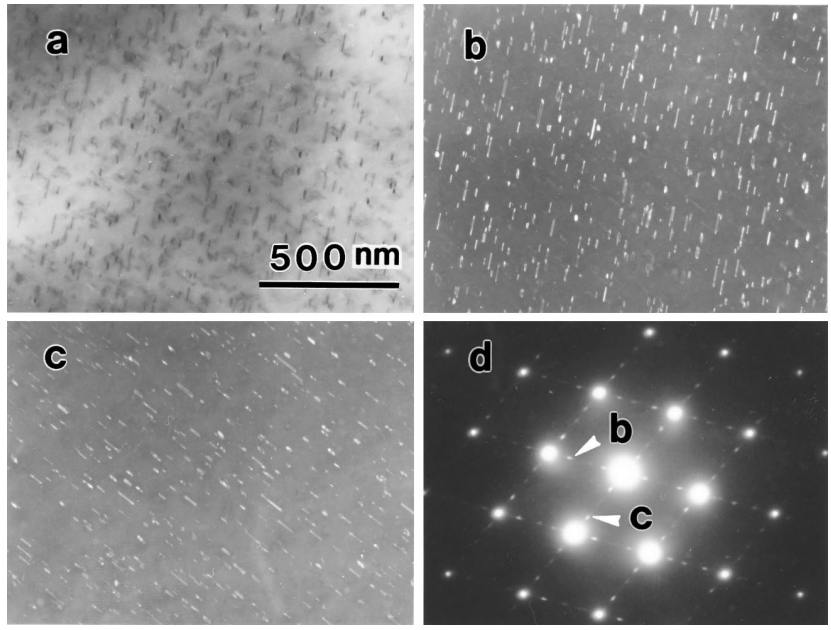

Fig. 5. TEM micrographs of Al_2O_3–3 mol%Ti_2O_3 aged at 1100°C for 24 h; (a) is the bright-field image, (b) and (c) are the dark-field images taken in the same area using the spots of b and c in the diffraction pattern of (d).

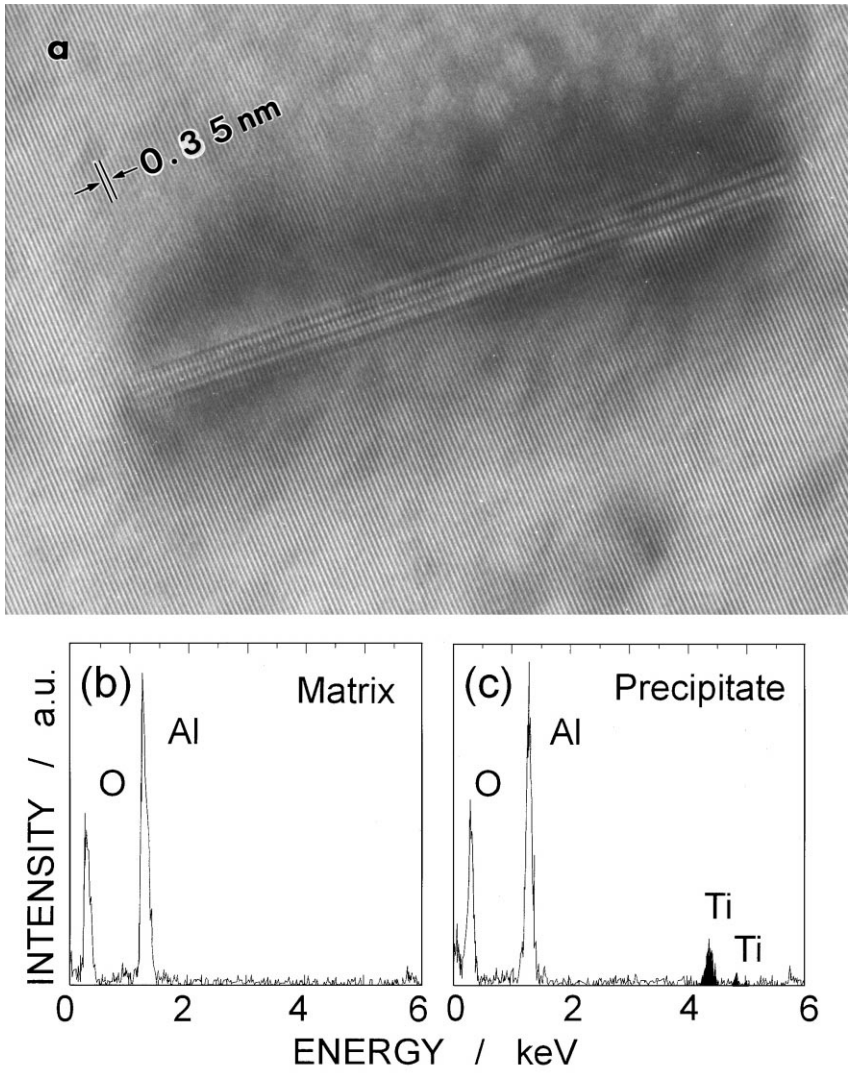

Fig. 6. A high-resolution electron micrograph of a nanoprecipitate in Al_2O_3–3 mol%Ti_2O_3 aged at 1100°C for 24 h (a) and the EDS profiles taken from matrix (b) and the precipitate (c), respectively. The probe diameter used for the EDS analysis is 10 nm.

trivalent to tetravalent state is not affected by diffusive flux of Ti^{4+} ions, which is very limited in α-Al_2O_3 as mentioned before. Oxidation will take place by producing either aluminum vacancy V_{Al}''' or interstitial oxygen O_i''. Judging from the defect formation energy,[9] V_{Al}''' will more easily be formed than O_i''. Since the vacancy diffusion is expected to occurs much rapidly than the lattice diffusion of Al^{3+} or O^{2-} ions, the oxidation will be induced fairly rapidly during ageing in oxidised atmosphere.

4 CONCLUSIONS

The solubility limit of Ti_2O_3 in Al_2O_3 is determined to be 1.3, 2.0, 3.0 and 3.7 mol% at 1400, 1500, 1600, 1700°C, respectively. The result is consistent with the microstructure change after heat treatment in Al_2O_3–3 mol% Ti_2O_3. Al_2O_3–3 mol% Ti_2O_3 sintered at 1600°C for 2 h in a reduced atmosphere of Ar–5%H_2 is single-phase solid solutions with corundum structure. After ageing at 1100°C for 24 h in the same reduced atmosphere, coarse Ti_2O_3 precipitates with an average size of about 500nm are formed inside grains due to the reduction in solubility of Ti^{3+} ions with temperature decrease. In contrast, a high density of nanoprecipitates with a size of 20∼80 nm are formed after ageing at 1100°C for 24 h in an oxidised atmosphere. They are not an equilibrium phase of TiO_2 with rutile structure but are metastable precipitates, which are fully coherent with α-Al_2O_3 matrix. The nanoprecipitation is expected to occur by valency change of titanium ions from trivalent to tetravalent during oxidation, and their thermal stability is related to a very limited solubility of Ti^{4+} ions in α-Al_2O_3.

ACKNOWLEDGEMENTS

The authors would like to thank Mr T. Kamino and Ms T. Yaguchi at Techono Research Laboratory of Hitachi Instruments Engineering Co., Ltd for their experimental assistance in high-resolution electron microscopy. Thanks are also due to Mr K. Banzai for his help in sample preparation.

REFERENCES

1. NIIHARA, K., HIRANO, T., NAKAHIRA, A., SUGANUMA, K., IZAKI, K. & KAWAKAMI, T., Nanostructure and thermomechanical properties of Si_3N_4/SiC composites fabricated from Si–C–N precursor powders. *J. Jpn Powd. Powd. Met.*, **36** (1989) 243–247.
2. NIIHARA, K., New design concept of structural ceramics–ceramic nanocomposites. *J. Ceram. Soc. Jpn*, **99** (1991) 974–982.
3. NAWA, M., SEKINO, T. & NIIHARA, K., Fabrication and mechanical behavior of Al_2O_3/Mo nanocomposites. *J. Mater. Sci.*, **29** (1994) 3185–3192.
4. MOON, A. R. & PHILIPS, M. R., Iron and spinel precipitation in iron-doped sapphire. *J. Am. Ceram. Soc.*, **74** (1991) 865–868.
5. BACKHAUS-RICOULT, M., HAGÉGE, S., PEYROT, A. & MOREAU, P., Internal reduction of chromium-doped α-alumina. *J. Am. Ceram. Soc.*, **77** (1994) 423–430.
6. ROUSSET., A., Alumina–metal (Fe, Cr, $Fe_{0.8}$ $Cr_{0.2}$) nanocomposites. *J. Solid State Chem.*, **111** (1994) 164–171.
7. HANDWERKER, C. A., FOECKE, T. J., WALLANCE, J. S., KATINER, U. R. & JIGGETS, R. D., Formation of alumina–chromium composites by a partial reduction reaction. *Mater. Sci. Engg. A*, **195** (1995) 89–100.
8. MCKEE Jr, W. D. & ALESHIN, E., Aluminum oxide–titanium oxide solid solution. *J. Am. Ceram. Soc.*, **46** (1963) 54–58.
9. GRIMES, T. W., Solution of MgO, CaO, and TiO_2 in α-Al_2O_3. *J. Am. Ceram. Soc.*, **77** (1994) 378–384.
10. LIFSHITZ, I. M. & SLYOZOV, V. V., The kinetics of precipitation from supersaturated solid solutions. *J. Phys. Chem. Solids*, **19** (1961) 35–50.
11. WAGNER, C., Theorie der alterung von niederschlagen durch umlösen. *Zeit. f. Elektrochem.*, **65** (1961) 581–591.